

# A new approach to optimize the energy efficiency of CO<sub>2</sub> transcritical refrigeration plants

*Ignacio Peñarrocha<sup>1</sup>, Rodrigo Llopis<sup>2,\*</sup>, Luis Tárrega<sup>1</sup>,  
Daniel Sánchez<sup>2</sup>, Ramón Cabello<sup>2</sup>*

*<sup>1</sup>Jaume I University, Dep. of Industrial Systems Engineering and Design, Campus de Riu Sec s/n  
E-12071, Castellón, Spain*

*<sup>2</sup>Jaume I University, Dep. of Mechanical Engineering and Construction, Campus de Riu Sec s/n  
E-12071, Castellón, Spain*

\*Corresponding author: Rodrigo Llopis ([rllopis@uji.es](mailto:rllopis@uji.es)), Phone: +34 964 72 8136; Fax: +34 964 728106.

## ABSTRACT

This paper proposes a model-free real-time optimization and control strategy for CO<sub>2</sub> transcritical refrigeration plants that assures covering the cooling demand and continuous tracking of conditions for maximum efficiency. Our approach obtains the feedback with only three measurements, and controls the opening degree of a back-pressure valve and the speed of the compressor. The strategy minimizes the power consumption of the compressor instead of maximizing the coefficient of performance, which avoids several sensors, and we demonstrate mathematically that both approaches are equivalent. We implemented the strategy with an algorithm that includes two independent auto tuned controllers, one devoted to regulate the high-pressure and another to regulate the outlet temperature of the secondary fluid of the evaporator. It also incorporates a real time perturb and observe procedure to locate on-line the optimum high-pressure that minimizes the compressor power consumption. The paper presents the experimental evaluation of the control strategy, verifying the stable operation of the algorithm and the energy optimization of the plant.

## KEYWORDS

CO<sub>2</sub>; transcritical; control; high-pressure optimization.

## NOMENCLATURE

---

$a_i$	coefficient of adjustment
$C$	Controller
$COP$	coefficient of performance
$c_p$	specific isobaric heat, $\text{kJ}\cdot\text{kg}^{-1}\cdot\text{K}^{-1}$
$d_i$	coefficient of adjustment
$E$	Error
$H$	specific enthalpy, $\text{kJ}\cdot\text{kg}^{-1}\cdot\text{K}^{-1}$
$K_p$	proportional term of the PI controller
$\dot{m}$	mass flow rate, $\text{kg}\cdot\text{s}^{-1}$
$N$	compressor speed, rpm
$O$	Optimizer
$OD$	opening degree of the electronic expansion valve, %
$P$	pressure, bar
$P_c$	compressor power consumption, kW
$P_e$	electrical power consumption, kW
$\dot{Q}_o$	cooling capacity, kW
$RP$	refrigeration plant
$R_{\text{tot}}$	total degree of superheat at compressor suction, K
$t$	time, s
$T$	temperature, K
$T_i$	integral time of the controller, s
$u$	control action to regulate the compressor speed
$v$	control action to regulate the opening degree of the expansion valve
$\dot{V}_n$	nominal displacement of the compressor, $\text{m}^3\cdot\text{s}^{-1}\cdot\text{rpm}^{-1}$

## Greek symbols

---

$\alpha$	constant of the isentropic efficiency of the compressor
$\beta$	slope of the isentropic efficiency of the compressor
$\gamma$	constant of the volumetric efficiency of the compressor

$\delta$	slope of the volumetric efficiency of the compressor
$\epsilon$	step of high-pressure used by the optimizer
$\eta_{me}$	mechanical-electrical efficiency
$\eta_i$	isentropic efficiency of the compressor
$\eta_v$	volumetric efficiency of the compressor
$v$	specific volume, $\text{m}^3 \cdot \text{kg}^{-1}$

### Subscripts

---

<i>dem</i>	Demand
<i>env</i>	environment temperature
<i>gc</i>	gas-cooler
<i>h</i>	high-pressure of the cycle
<i>in</i>	Inlet
<i>l</i>	low pressure of the cycle
<i>o</i>	Outlet
<i>p</i>	Pressure
<i>sf</i>	secondary fluid
<i>sp</i>	setpoint
<i>T</i>	Temperature
<i>w</i>	Water

## 1. INTRODUCTION

Transcritical carbon dioxide refrigeration systems have been implemented in the last decade, especially in supermarket refrigeration, where some plants are in operation [1], particularly in European northern countries where the low ambient temperatures allow this type of systems to operate most of the time under subcritical operation. However, when referring to warm and hot countries, these systems operate more time in supercritical conditions, what delays its implementation.

The most critical point in the operation of CO<sub>2</sub> transcritical refrigeration plants is the exit of the gas-cooler, where temperature and pressure are independent variables [2]. This independence makes the COP depend on the high operating pressure. An optimum value of this pressure that maximizes COP exists and it depends on the refrigerant outlet temperature of the gas-cooler and on the evaporating level, as analysed by several researchers. Cabello et al. [3] presented a critical analysis, based on experimental data, of the relations for calculating this optimum pressure, and concluded that the expressions of Liao et al. [4] and Sarkar et al. [5] fitted better the behaviour of a single-stage plant.

The CO<sub>2</sub> most widespread system in supermarket refrigeration [6], excluding the cascade systems, incorporates a two-stage expansion system that allows controlling the high-pressure and the outlet conditions at the exit of the evaporator (see Figure 1). A back-pressure or a differential pressure valve usually does the first function, whereas electronic expansion valves working as thermostatic valves usually does the second. The accumulation tank appears commonly between those regulation devices. Also, this cycle can incorporate internal heat exchangers [7] and operate in transcritical and subcritical conditions [8].

Figure 1. Transcritical refrigeration CO<sub>2</sub> cycle with double expansion and P-h diagram

The COP dependence on the high operating pressure and the need of upgrading the energy efficiency of these systems motivated several authors to investigate about different control strategies in CO<sub>2</sub> transcritical refrigeration plants. Ge & Tassou [9] analysed, from a theoretical view, a control strategy of the high-pressure of a CO<sub>2</sub> medium temperature retail food refrigeration system. Their strategy allowed the plant to operate in either transcritical or subcritical conditions and they focused on the transitional temperature between both regimes. Cecchinato *et al.* [10] centred their study in a chiller producing propylene-glycol at -8°C. In addition, they studied theoretically and experimentally, the transition between subcritical and transcritical conditions. On the other side, Agrawal & Bhattacharyya [11] analysed

experimentally the performance of capillary tubes against controllable expansion valves for a heat pump system. They concluded that the capillary tubes allow obtaining the same COP levels as the controllable valves especially at high gas-cooler temperatures. Casson *et al.* [12] analysed theoretically two different throttling systems considering a plant operating in transcritical conditions.

The above-mentioned works focused on the optimization of concrete refrigeration and heat pump cycles. However, other researchers considered generic control strategies valid for each refrigeration system, and avoided experimentation with specific refrigeration plants. First, Aprea & Maiorino [13], from the ideas of Liao *et al.* [4], generalized the optimum high-pressure correlation by using two adjusting parameters of the isentropic efficiency of the compressors. With the measurements of the evaporating temperature, the outlet gas-cooler refrigerant temperature, and the pressure at the gas-cooler approximated the optimum pressure. This strategy cannot check if the plant is running in conditions of maximum efficiency, since no energy feedback is possible. Second, Zhang and Zhang [14] proposed a regulation strategy applicable in any CO<sub>2</sub> transcritical refrigeration plant with only four cycle parameters: the temperatures of the refrigerant at compressor suction and at outlet of the gas-cooler, and the pressures at the exit of the gas-cooler and at the compressor discharge. This strategy obtains the feedback by computing the approximate COP value for each instant using the four measurements and by means of a steepest descent method readjusts the pressure at the gas-cooler to find out the optimum conditions. The work addressed theoretically the approach, but not experimentally.

Based on the previous works, we miss general optimization approaches independent of COP and high-pressure mathematical relationships and energy feedback to check on-line the validity of the operation point. In this work, we do not track the optimal high-pressure given by a mathematical expression, but we look continuously for the minimum power consumption. We obtain and test a widespread procedure for fast tracking of the conditions for maximum efficiency. We propose an approach whose main features are the use of a reduced number of sensor elements, the adaptability of the controller adjustment leading to independency of the refrigeration cycle and its components, and the guarantee of operating the plant in conditions of maximum efficiency. This paper demonstrates mathematically the validity of the approach, details the implementation procedure and its experimental verification in a transcritical CO<sub>2</sub> refrigeration plant devoted to provide secondary fluid in the evaporator at a determinate temperature, similar to the operation of water chillers used for air conditioning.

## 2. OPTIMIZATION ANALYSIS

The objective of a control mechanism in transcritical refrigeration plants is to provide the required cooling capacity with the maximum possible energy efficiency. In the case of transcritical plants, it means to operate the cycle with the pressure at the gas-cooler (high-pressure) that provides the maximum COP.

The COP of the cycle of Figure 1 is the quotient between the cooling capacity provided by the cycle ( 1 ) and the compressor power consumption( 2 ) as expressed by equation ( 3 ).

$$\dot{Q}_o = \dot{m} \cdot (h_1 - h_4) \quad (1)$$

$$P_c = \dot{m} \cdot (h_2 - h_1) \quad (2)$$

$$COP = \frac{\dot{Q}_o}{P_c} = \frac{h_1 - h_4}{h_2 - h_1} \quad (3)$$

Thus, to optimize the energy performance, expression ( 3 ) must be maximized. If we differentiate equation ( 3 ) after expressing the enthalpies as a function of the high-pressure, we can obtain the mathematical expression of the high-pressure that maximizes the COP. For an operation point of the plant, determined by a fixed evaporation level and fixed properties of the refrigerant at the compressor suction, we evaluate the compressor discharge enthalpy with the properties of the refrigerant at suction as expressed by relation ( 4 ), where  $\eta_i = \alpha - \beta \cdot \frac{P_h}{P_l}$  is the isentropic efficiency of the compressor.

$$h_2 = h_1 + \frac{h_{2,s} - h_1}{\eta_i} = h_1 + \frac{h_{2,s} - h_1}{\alpha - \beta \cdot \frac{P_h}{P_l}} \rightarrow h_2 = d_0 + d_1 \cdot P_h \quad (4)$$

After an analysis of experimental data we observed that the compressor discharge enthalpy ( $h_2$ ) can be represented by a linear function of the high-pressure ( 4 ), where the coefficients  $d_i$  depend on the compressor characteristics.

Moreover, the enthalpy at the exit of the gas-cooler depends on its temperature and the high-pressure, and we represent it by the polynomial function ( 5 ).

$$h_3 = a_0(T) + a_1(T) \cdot P_h + a_2(T) \cdot P_h^2 + a_3(T) \cdot P_h^3 \quad (5)$$

We consider a third order polynomial that fits accurately the real function, although higher orders are also valid. The coefficients  $a_i$  depend on the gas-cooler outlet temperature.

Finally, we consider the expansion process isenthalpic and no energy losses in the expansion process, what equals the inlet enthalpy of the evaporator to the outlet enthalpy of the gas-cooler.

Using the approximate relations for the enthalpies, we write COP as a function of the high-pressure as ( 6 ).

$$COP = \frac{\dot{Q}_o}{P_c} = \frac{h_1 - (a_0(T) + a_1(T) \cdot P_h + a_2(T) \cdot P_h^2 + a_3(T) \cdot P_h^3)}{d_0 + d_1 \cdot P_h - h_1} \quad (6)$$

Then, differentiating equation ( 6 ) with respect to the high-pressure and equalling the result to zero, we obtain the high-pressure values that maximize the COP, as expressed by ( 7 ).

$$\frac{dCOP}{dP_h} = 0 \quad (7)$$

The implicit relation that provides the COP optimum values from ( 7 ), results in ( 8 ).

$$\begin{aligned} & \frac{a_1(T) + 2 \cdot a_2(T) \cdot P_h + 3 \cdot a_3(T) \cdot P_h^2}{d_0 + d_1 \cdot P_h - h_1} \\ & + \frac{d_1 \cdot (a_0(T) + a_1(T) \cdot P_h + a_2(T) \cdot P_h^2 + a_3(T) \cdot P_h^3)}{(d_0 + d_1 \cdot P_h - h_1)^2} = 0 \end{aligned} \quad (8)$$

Relation ( 8 ) shows that the optimum high-pressure values only depend on the conditions of the refrigerant at compressor suction, the characteristics of the compressor and the temperature at the outlet of the gas-cooler, and not on the compressor speed, as Liao et al. [4] and Sarkar et al. [5] showed, and as Cabello et al. [3] verified experimentally.

Zhang & Zhang [14] analysed theoretically a regulation strategy in which they measured at least three temperatures and two pressure values (to evaluate the outlet enthalpies of the evaporator and gas-cooler and at the compressor suction and discharge) and then computed the COP with ( 3 ) to update the high-pressure value depending on the COP trend. They proposed another algorithm using two temperature and two pressure sensors, but they stated that this simplification deviate the COP to values under its optimum.

We search for an alternative optimization of the plant independent of theoretical expressions of the relationship between COP and high-pressure, avoiding real deviations of these equations and the sensors that lead to the COP computation. We obtain cycle information and guarantee maximum efficiency conditions minimizing the compressor power consumption (instead of maximizing the COP) and ensuring that the cycle fulfils the cooling demand at the same time. Mathematically, we express this optimization problem as ( 9 ).

$$\left. \begin{aligned} & \min(P_c) \\ & \text{subject to } (\dot{Q}_o = \dot{Q}_{dem}) \end{aligned} \right\} \quad (9)$$

We must first derive the compressor power consumption and cooling capacity to obtain the solution of the optimization problem ( 9 ). We express the refrigerant mass flow rate through the compressor as a function of the compressor speed  $N$ , the properties of the refrigerant at suction and the volumetric efficiency of the compressor  $\eta_v$ , leading to ( 10 ).

$$\dot{m} = \frac{N \cdot \dot{V}_n}{v_1} \cdot \eta_v = \frac{N \cdot \dot{V}_n}{v_1} \cdot \left( \gamma - \delta \cdot \frac{P_h}{P_l} \right), \quad (10)$$

Combining equations ( 2 ) to ( 5 ) and ( 10 ), we write the cooling capacity and the compressor power consumption as ( 11 ) and ( 12 ) respectively.

$$\dot{Q}_o = \frac{N \cdot \dot{V}_n}{v_1} \cdot \left( \gamma - \delta \cdot \frac{P_h}{P_l} \right) \cdot [h_1 - (a_0(T) + a_1(T) \cdot P_h + a_2(T) \cdot P_h^2 + a_3(T) \cdot P_h^3)] \quad (11)$$

$$P_c = \frac{N \cdot \dot{V}_n}{v_1} \cdot \left( \gamma - \delta \cdot \frac{P_h}{P_l} \right) \cdot [(d_0 + d_1 \cdot P_h - h_1)] \quad (12)$$

Using relations ( 11 ) and ( 12 ), the optimization problem defined by ( 9 ) results in ( 13 ).

$$\left. \begin{array}{l} \max \left\{ -\frac{N \cdot \dot{V}_n}{v_1} \cdot \left( \gamma - \delta \cdot \frac{P_h}{P_l} \right) \cdot [(d_0 + d_1 \cdot P_h - h_1)] \right\} \\ \text{sub. to } \left\{ \frac{N \cdot \dot{V}_n}{v_1} \cdot \left( \gamma - \delta \cdot \frac{P_h}{P_l} \right) \cdot [h_1 - (a_0(T) + a_1(T) \cdot P_h + a_2(T) \cdot P_h^2 + a_3(T) \cdot P_h^3)] = \dot{Q}_{dem} \right\} \end{array} \right\} \quad (13)$$

Now, consider that the compressor speed and the high-pressure are the manipulable variables in the plant, and consider that it operates at an evaporating level with fixed properties of the refrigerant at compressor suction. Then, the optimization problem determined by ( 13 ) and solved using the Lagrange Multiplier Method [15], offers the compressor speed and the high-pressure values assuring the cooling demand with minimum power consumption as expressed by ( 14 ) and ( 15 ).

$$N = \dot{Q}_{dem} \cdot \frac{v_1}{\dot{V}_n \cdot \left( \gamma - \delta \cdot \frac{P_h}{P_l} \right) \cdot [h_1 - (a_0(T) + a_1(T) \cdot P_h + a_2(T) \cdot P_h^2 + a_3(T) \cdot P_h^3)]} \quad (14)$$

$$\frac{(d_0 + d_1 \cdot P_h - h_1) \cdot (a_1(T) + 2 \cdot a_2(T) \cdot P_h + 3 \cdot a_3(T) \cdot P_h^2)}{h_1 - (a_0(T) + a_1(T) \cdot P_h + a_2(T) \cdot P_h^2 + a_3(T) \cdot P_h^3)} + d_1 = 0 \quad (15)$$

We observe from ( 15 ) and ( 8 ) that the optimum high-pressure value only depends on the properties of the refrigerant at the suction, the compressor and the outlet temperature of the refrigerant at the gas-cooler.

Finally, we must demonstrate that solution of equation ( 8 ) (from maximizing the COP) is equal to that of relation ( 15 ) (minimizing the compressor power consumption) to check the validity of the approach. Figure 2 shows this comparison for an evaporating level of 35bar with a superheating degree at compressor suction of 15°C, for two gas-cooler outlet temperatures. It shows the COP evolution ( 6 ), its



differential relation ( 8 ) and the result of the optimization method ( 15 ). Both differential relations ( 8 ) and ( 15 ) locate the same optimum high-pressure value, which matches with the maximum COP offered by relation ( 6 ).

Figure 2. COP and equations ( 8 ) and ( 15 ) evolutions for  $P_o=35\text{bar}$  with  $R_{tot}=15^\circ\text{C}$  at two gas-cooler outlet temperatures

Thus, we demonstrate mathematically that the proposed optimization strategy, minimizing the power consumption of the compressor subject to fulfil the cooling demand, is equivalent to maximizing the COP. Therefore, this strategy is useful for optimizing the performance of  $\text{CO}_2$  refrigeration transcritical plants.

This control method of  $\text{CO}_2$  transcritical refrigeration plants applies for systems whose cooling demand is known, using equations ( 14 ) and ( 15 ). However, in refrigeration applications the cooling capacity is generally unknown and difficult to measure it. For example in water chillers, we usually measure the temperature of the secondary fluid at the outlet of the evaporator. The cooling demand is a function of the secondary fluid inlet temperature at the evaporator and its mass flow rate

$$\dot{Q}_{dem} = \dot{m}_{sf} \cdot c_{p,sf} \cdot (T_{sf,in} - T_{sf,o}). \quad (16)$$

Accordingly, we implement the control method taking as reference variable the temperature of the secondary fluid at the exit of the evaporator and considering as disturbance variables the secondary fluid inlet temperature at the evaporator and its mass flow rate. This approach is the common form of water chillers operation, whose objective is to achieve a determinate reference outlet temperature of the secondary fluid at the evaporator. Thus, the proposed method applies with the same accuracy in transcritical refrigeration plants providing a temperature at the exit of the evaporator equal to a reference temperature.

To sum up, this control method is useful, for example, to optimize the energy performance of chillers using a low number of sensors ensuring that they operate in conditions of maximum COP. The needed feedback in this case would only be the compressor power consumption, the high-pressure and the outlet temperature of the secondary fluid of the evaporator.

In section 3 the implementation of the proposed optimization algorithm is analysed and presented.

### 3. CONTROL SYSTEM CONFIGURATION

Different combinations of the compressor speed  $N$  and high-pressure  $P_h$  can drive the refrigeration system to a temperature  $T_{sf,o} = T_{sf,sp}$  under fixed conditions of gas-cooler outlet temperature  $T_{gc,o}$ , secondary fluid mass flow  $\dot{m}_{sf}$  and its temperature  $T_{sf,in}$ . However, only one combination leads to the minimum power consumption. As  $T_{gc,o}$ ,  $\dot{m}_{sf}$  and  $T_{sf,in}$  vary continuously over time, we must adapt the values of  $N$  and  $P_h$  to each new situation. If we knew exactly the values of  $T_{gc,o}$ ,  $\dot{m}_{sf}$ ,  $T_{sf,in}$  and the parameters of the plant at each instant of time (assuming that the previous model had no uncertainty), then we could drive continuously the plant to the exact values of  $N$  and  $P_h$  leading to the desired temperature  $T_{sf,sp}$  with the minimum power consumption. Aprea & Mariorino [13] and Zhang & Zhang [14] dealt the optimization problem with experimental expressions of the optimum high-pressure. The resources needed to obtain tight empirical expressions make that approach impractical for a generalization of an optimization procedure. Furthermore, even if we obtain tight expressions, the number of sensors needed to implement a real-time optimization procedure increases the cost of the optimizer.

We did not find on the literature a general control and optimization procedure for these plants that avoids the use of a previous model and at the same time minimizes implemented technology (sensors and actuators). This section addresses the development of a general control and optimization strategy applicable to any refrigeration plant operating with CO<sub>2</sub> in transcritical conditions.

The goals of the control system are to assure: (i) a constant temperature of the secondary fluid at the evaporator outlet  $T_{sf,o} = T_{sf,sp}$ ; (ii) minimum power consumption  $P_c$ ; (iii) pressure values within the allowed limits for (safe) operation on transcritical region; and (iv) robustness in the presence of time varying gas-cooler outlet temperature  $T_{gc,o}$ , and time varying values of  $T_{sf,in}$  and  $\dot{m}_{sf}$ . The robustness to the presence of the mentioned disturbances refers to the desire of a fast adaptation for the new optimum operating point when the external conditions change (mainly dependent on the environmental temperature). We include the following actuators in the system to achieve these goals.

First, we include a variable-frequency driver (VFD) to manipulate the rotational speed of the compressor. It receives as an input signal the desired rotational speed on the compressor ( $u$ ) and its internal control loop decides the supply voltage of the machine to achieve the desired rotational speed (i.e., to achieve that

$u = N$ ). This internal controller is common in all VFD and is out of the scope of this work, and we assume that it is properly tuned. The VFD gives as a measurable output signal the electrical power consumption ( $P_e$ ) that is proportional to the mechanical power  $P_c$  through the electromechanical efficiency  $\eta_{me}$  of the power electronics and mechanical behaviour of the compressor (17). We thus acquire this signal without an additional sensor.

$$P_e = \frac{P_c}{\eta_{me}} \quad (17)$$

Second, we include an electronic expansion valve with a servomotor (also named controlled servo valve) to manipulate the back-pressure valve involved in the operating high-pressure. These valves include commonly a stepper motor or a servomotor, being the ones with stepper motor less expensive with accuracy enough for our application. A commercial power drive usually integrated with the controlled servo valve drives this stepper motor. It receives the number of steps that the stepper motor must move as an input signal (let us call it  $v$ ). Each movement of the stepper motor causes a different opening degree (OD) in the back-pressure valve, modifying in this way the high-pressure, among other variables in the system. We must manipulate the stepper motor assuring a high-pressure bounded between some prescribed values; this assures safety behaviour of the machine and operation on the transcritical region. For this reason, we also include a pressure sensor of the high-pressure  $P_h$ .

Finally, we measure the temperature  $T_{sf,o}$  through a temperature sensor, like a thermocouple or a thermo resistance to control the refrigeration system with the required performance.

We implement the optimal controller in a processor-based platform with peripherals to acquire and generate signals (as, for instance, a microcontroller or a programmable logic controller). This platform uses of the three measured signals  $T_{sf,o}$ ,  $P_e$  and  $P_h$  to decide at each instant of time the values of the desired rotational speed of the compressor  $u$  and the position of the stepper motor  $v$  that modifies the back-pressure OD so that the reference temperature remains constant with the minimum possible power consumption.

Figure 3 shows the inclusion of the mentioned actuators, sensors and control unit together to the refrigeration plant. Figure 4 shows a block diagram with the refrigeration plant (that includes the actuators and sensors) and the feedback controller. It also includes the manipulated inputs ( $u$  and  $v$ ), the measured outputs ( $T_{sf,o}$ ,  $P_e$  and  $P_h$ ), the non-measured disturbances that affect the behaviour of the plant at each instant of time ( $T_{env}$ ,  $T_{sf,in}$  and  $\dot{m}_{sf}$ ), as well as the setpoint for the desired temperature  $T_{sf,sp}$ .

Figure 3. Scheme of the refrigeration plant, actuators, measured and control signals

Figure 4. Control scheme of the refrigeration plant

#### 4. DESIGN OF THE OPTIMIZATION AND CONTROL ALGORITHM

We choose a “perturb and observe” approach (P&O) for the optimizer to avoid the need of a model of the plant. The P&O approaches consists on modifying the steady state of the plant periodically, and then decide further modifications based on the new achieved power consumption. We present different approaches that modify the state of the plant. Figure 5 shows the easiest optimization approaches, those that modify directly one of the control actions of the system and let the other one given by a temperature controller  $\mathcal{C}$  (note that  $P_h$  is unmeasured).

Figure 5. Possible schemes to regulate the secondary fluid outlet temperature and the power consumption of the refrigeration plant

In the first scheme, the optimizer  $\mathcal{O}$  perturbs the plant fixing periodically a new value of the opening degree of the back-pressure valve ( $v$ ). A temperature controller ( $\mathcal{C}_T$ ) changes continuously the compressor speed (by means of  $u$ ) to assure that the outlet temperature of the secondary fluid is kept close to  $T_{sf,sp}$  for the fixed opening degree. Once it achieves a new steady state, the optimizer  $\mathcal{O}$  fixes a new opening degree depending on the achieved consumption (i.e., the observation).

In the second scheme, the optimizer  $\mathcal{O}$  fixes periodically a new value (perturbs) for the compressor speed  $u$ , and the controller  $\mathcal{C}_T$  modifies continuously the opening degree  $v$  to keep the outlet temperature constant. Once it achieves a new steady state, the optimizer  $\mathcal{O}$  decides a new compressor speed based on the new value of the power consumption (i.e., the observation).

The optimization algorithm to be applied in optimizer  $\mathcal{O}$  with the first scheme is as follows: First let us assume that the system is in steady state at instant  $k$  with some values  $v = v_k$  and  $P_e = P_{e,k}$ , and take some prescribed value  $\epsilon$  (let us call it seeking parameter). Then, follow these steps indefinitely:

1. Set  $k = k + 1$ , and set the new control action as  $v_k = v_{k-1} + \epsilon$ .
2. Wait until the system achieves a new steady state.

3. Compare the new power consumption  $P_{e,k}$  with the previous achieved one:  $P_{e,k-1}$ . If you improved this value (i.e., if  $P_{e,k} < P_{e,k-1}$ ), then go to Step 1. If it is not, then set  $\epsilon = -\epsilon$  and go to Step 1.

Note that this kind of algorithm achieves an oscillatory behaviour around the optimal point as it is always changing the steady state. However, this leads to the ability of the algorithm to detect changes on the power consumption due to the exogenous disturbances. One of the advantages of this approach is avoiding the use of the high-pressure sensor, but it has two main drawbacks. (i) It does not assure that the pressure at each step reaches a value within the allowed range of operation (safe and transcritical). (ii) The time needed to achieve a steady state in Step 2 can be arbitrarily long, and, therefore, the desired ability of fast adaption to external disturbances (change on the temperature and cooling load) is lost.

We propose the cascade structure for the controller and optimizer (Figure 6) to avoid the drawbacks of the previous approach. Optimizer  $\mathcal{O}$  uses the power consumption measurement to decide the high-pressure operating setpoint  $P_{h,sp}$  that leads to an optimal and safe behaviour. The algorithm in the optimizer differs from the previous one in that manipulates  $P_{h,sp,k}$  instead of  $v_k$ . The controller  $\mathcal{C}$  uses the available measurements of the temperature and pressure to decide the control to achieve and keep constant the demanded values of temperature and high-pressure.

Figure 6. Cascade structure for the controller and optimizer

We need a dynamical multivariable controller  $\mathcal{C}$  able to achieve the references as fast as possible and without permanent error because the refrigeration plant has a dynamical behaviour with non-depreciable transient time. We appreciate this slow dynamics in response to changes on the compressor speed and on the opening degree of the back-pressure valve, as well on changes on the thermal load and environment temperature  $T_{env}$ . We choose a decoupled control strategy with the aim of obtaining a simple tuning procedure and implementation of this controller. We split the controller  $\mathcal{C}$  into two independent controllers where each one tracks just one of the variables and manipulates just one of the control actions. We first analyse the availability of change of the system (i.e., the gain) from each control action ( $u$  and  $v$ ) to each output ( $T_{sf,o}$  and  $P_h$ ) to make the correct chose of pairing between controlled and manipulated variables that leads to the most accurate and fastest possible response [16]. This behaviour depends on the available range of the actuators chosen in the installation, but, when we choose them with proper dimensions, the behaviour explained next is what usually happens in practice.

Consider that the plant is operating in steady state at an operation point defined by  $N(t_0)$ ,  $OD(t_0)$ ,  $T_{sf,o}(t_0)$  and  $P_h(t_0)$  with constant disturbances, and then we apply a step change in the compressor speed while keeping constant the opening degree of the back-pressure valve. Then, after a transient time, the system will achieve a new steady state with new values  $N(t_1)$ ,  $T_{sf,o}(t_1)$  and  $P_h(t_1)$ . If we express the observed change of each of the outputs in relative terms with respect of their possible range variation and as a function of the speed variation (in relative terms), then we observe empirically the following approximated behaviour

$$\frac{T_{sf,o}(t_1) - T_{sf,o}(t_0)}{T_{sf,o,range}} \approx -1 \cdot \frac{N(t_1) - N(t_0)}{N_{range}}, \quad (18)$$

$$\frac{P_h(t_1) - P_h(t_0)}{P_{h,range}} \approx 0.1 \cdot \frac{N(t_1) - N(t_0)}{N_{range}}. \quad (19)$$

The sub index “range” refers to the available range of variation of each of the signals. If we carry out the same experiment with a step change on the opening degree but keeping constant the compressor speed, then we observe empirically the following approximate relations

$$\frac{T_{sf,o}(t_1) - T_{sf,o}(t_0)}{T_{sf,o,range}} \approx -0.1 \cdot \frac{OD(t_1) - OD(t_0)}{OD_{range}} \quad (20)$$

$$\frac{P_h(t_1) - P_h(t_0)}{P_{h,range}} \approx 1 \cdot \frac{OD(t_1) - OD(t_0)}{OD_{range}} \quad (21)$$

In practice, the incremental changes depend on the initial state due to the nonlinear behaviour of the plant, specially, due to the back-pressure valve, leading to complex relations. The expressions show that the variation of the compression speed affects significantly most to variations on the temperature than the modification of the opening degree of the valve does. In addition, the opening degree variations affect more to variations on the high-pressure than the rotational speed does.

With this reasoning, we implement two independent controllers, one tracking the desired temperature and actuating over the rotational speed of the compressor (controller  $\mathcal{C}_T$ ), and the other one tracking the high-pressure actuating over the opening degree of the back-pressure valve (controller  $\mathcal{C}_P$ ). Figure 7 shows the resulting control scheme. If we find the above gains higher with the other possible pairing, then we must interchange the control actions.

Figure 7. Final control structure of the plant with the optimizer

We propose a proportional-integral (PI) strategy [17] to minimize the number of tuning parameters and to avoid the negative effects of the measurement noise. The following law defines the PI control strategy for the temperature controller:

$$e_T(t) = T_{sf,sp} - T_{sf,o} \quad (22)$$

$$u(t) = K_{p,T} \left( e_T(t) + \frac{1}{T_{i,T}} \int_0^t e_T(\tau) d\tau \right) \quad (23)$$

For the high-pressure controller the law reads as:

$$e_P(t) = P_{h,sp} - P_h \quad (24)$$

$$v(t) = K_{p,P} \left( e_P(t) + \frac{1}{T_{i,P}} \int_0^t e_P(\tau) d\tau \right) \quad (25)$$

The signals  $e_T(t)$  and  $e_P(t)$  are the instantaneous tracking errors that we desire to drive to zero as fast as possible. The four parameters  $K_{p,T}$ ,  $T_{i,T}$ ,  $K_{p,P}$ ,  $T_{i,P}$  will define the behaviour of the controlled system. These parameters will affect the transient time after changes of the references and the disturbances ( $\dot{m}_{sf}$ ,  $T_{sf,in}$  and  $T_{env}$ ), and the maximum tracking error during these variations. We choose an experimental Ziegler-Nichols tuning procedure [17] to obtain these parameters and to simplify the start-up of the approach, as is the most commonly one used in the PI controllers used in industry. It applies a relay-based control and measures the behaviour of the controlled outputs (the period and amplitude of the oscillations). This autotuning procedure runs just once, when the machine operates for the first time, or with each significant plant modification.

Discrete approximations of equations (21) to (24) implement the PI controllers with a period of one second, which is enough for the dynamics of the refrigeration plant. We change the second step used for the optimizer algorithm ("wait until a new steady state is achieved") by waiting a fixed amount of time (normally in the order of minutes), the one needed by the two controllers to achieve a new steady state. With this idea, we implement the final algorithm as two periodical routines that run with a different frequency. A first periodic task runs the controller routine with a period of one second and includes the two PI controllers that try to keep the secondary fluid outlet temperature and the high-pressure indicated by the optimizer. A second periodic task runs the optimizer each several minutes, its input is the consumed electrical power and it decides the new high-pressure setpoint. The optimizer routine requires some initial

value on the power consumption  $P_{e,0}$ , and a prescribed value of  $\epsilon$  (in bar) used for the seek on the optimal pressure. The steps that the optimizer routine runs at each period are:

1. Acquire the new power consumption  $P_{e,k}$  and compare it with the previous one  $P_{e,k-1}$ .
2. If it has grown up, i.e.,  $P_{e,k} > P_{e,k-1}$ , then set  $\epsilon = -\epsilon$ .
3. Set  $P_{h,sp,k} = P_{h,sp,k-1} + \epsilon$ .
4. If  $P_{h,sp,k} > P_{h,sp,max}$  or  $P_{h,sp,k} < P_{h,sp,min}$ , then set  $P_{h,sp,k} = P_{h,sp,k-1} - \epsilon$

The fourth step of the algorithm avoids setpoint pressures outside the safe operating margins of the plant. It also avoids the search on a wrong direction for long periods. We must chose the seeking parameter  $\epsilon$  big enough to track fast the variations on the thermal load and on the environmental temperature, but small enough to find accurately the optimal operating point. Therefore, the selection of the value  $\epsilon$  is a trade-off between accuracy and tracking ability.

One of the main differences of the proposed algorithm with others explained in the literature is that the number of sensors reduces to two, and that it does not depend on any parameter of the plant. Furthermore, the temperature control and the optimization are considered together, and we use PI controllers for the achievement of new high-pressures and outlet temperatures, reducing the time needed to achieve the optimal point. Finally, the autotuning procedure allows its application on any plant.

The proposed algorithm can delay the achievement of the optimum operating point with fast and long variations of the temperature  $T_{env}$ . For example, in a transient involving an abrupt reduction of the environmental temperature, the algorithm will detect an improvement on the electrical power consumption independently on the pressure direction, and it can evolve in the wrong direction during a transient time. The worst case is when one has to wait until the algorithm achieves the boundary of the allowed pressure and then changes the direction towards the optimum value (thanks to Step 4).



## 5. BRIEF DESCRIPTION OF THE REFRIGERATION PLANT

We tested the proposed control algorithm in an experimental transcritical CO<sub>2</sub> refrigeration plant (Figure 8) whose layout diagram is equivalent to that presented in Figure 1. A 4kW semi-hermetic single-stage vapour compressor drives the plant with a double stage expansion system (electronic back-pressure and electronic expansion valves), concentric counter-current gas-cooler and evaporator. A loop of water/ethylene-glycol mixture (50% by volume) provides the thermal load and a water loop performs the heat rejection. Reference [3] provides a detailed description of the plant, reference [18] particularizes the characteristics of the compressor and references [19, 20] describe the characteristics of the heat exchangers. The plant includes a Coriolis mass flow meter, 2 volumetric flow meters for the secondary fluids, 10 pressure gauges, 17 thermocouples and a digital wattmeter that allows to monitor its performance.

Figure 8. View of the experimental plant and main actuators

We tested the control and optimization algorithm with the following actuators: two electronic stepper expansion valves working in parallel mode as back-pressure (Figure 8) with a diameter of orifice of 1.6mm, a stroke of 1.4mm with an advance of 0.0025mm/step, and a commercial variable frequency drive of 5.5kW.

We measured the high-pressure with a 4-20mA piezoelectric pressure gauge (0-160bar) with a calibrated uncertainty of  $\pm 0.96$ bar. We registered the temperature of the secondary fluid at the evaporator outlet with an immersion T-type thermocouple with a calibrated uncertainty of  $\pm 0.5$ °C. We measured the power consumption with the inverter drive of the compressor, and checked that value with the measurement from a digital wattmeter with an uncertainty of  $\pm 0.5$ %.

We gathered all the information with a SCXI data acquisition system and we implemented the control algorithm using a LabView-based application [21] that manipulates the electronic expansion valves and the compressor driver using 0-10VDC analogical signals.

## 6. EXPERIMENTAL RESULTS

In this section, we present and discuss the experimental results obtained after applying the proposed approach.

### 6.1. Autotuning

Figure 9 shows the autotuning procedure for the PI controllers. They need about 6.30 minutes, including the initial transient, to achieve a stable behaviour and to perform the two relay control experiments for each of the pairs ( $N$  with  $T_{sf,o}$  and  $OD$  with  $P_h$ ). Once the autotuning is finished, we set the setpoints  $T_{sf,sp} = 7^\circ\text{C}$ , and  $P_{h,sp} = 91.2$  bar. We decreased  $P_{h,sp}$  after minute 11.30 of the experiment, and obtained an establishing time of 5 minutes for the temperature controller, and 2 minutes for the high-pressure controller. In other operation conditions this transient times can be different.

Figure 9. Autotuning test for the PI controllers of the expansion valve and the compressor speed

During the autotuning experiment, we must excite significantly the plant and assure at the same time an operation inside the security margins. This implies an initial analysis of the plant to guess the relay values that fulfil these tradeoffs. We choose 1100 rpm for the compressor and relay amplitude of 300 rpm, which is inside of the allowable margins (see Figure 9). This implies high-pressures below 110 bar (security limit of the plant), and variations sufficiently high in the outlet temperature of the secondary fluid to adjust the PID parameters. We choose a 65% opening degree in the valve, and relay amplitude of 15%, leading to variations high enough to adjust the second PID controller, and to assure a pressure below 110 bar.

Although this autotuning procedure seems abrupt, we run it only once in the lifetime of the plant, or at least few times, and, accordingly, we consider its impact on the lifetime of the plant negligible. This procedure contrasts with the classical identification procedures with previous analysis of the plant, which need more time than the proposed one.

## 6.2. Real time optimization

Once the PID controllers are tuned, they run together with the optimization algorithm of section 4 to find the combination of  $N$  and  $OD$  that leads to temperature  $T_{sf,o} = 7^{\circ}C$  at the same time that minimizes the power consumption. We chose a value of  $\epsilon = 1\text{bar}$ .

Figure 10 shows the optimizer behaviour in a long time assay. In this assay, of 12 hours long, the inlet temperature of the water to the gas-cooler ( $T_{w,in}$ ) decreases from  $37.5^{\circ}C$  to  $34.2^{\circ}C$  approximately and the secondary fluid volumetric flow rates remain constant. The decrease of the inlet temperature of water to the gas-cooler is equivalent to a reduction of the environment temperature for a plant cooled with air. Figure 10 shows that the temperature controller achieves a constant temperature of the secondary fluid of  $7^{\circ}C$  manipulating the compressor speed. At the same time, the optimizer fixes a new pressure each 5 minutes with changes of  $\epsilon = 1\text{bar}$  up or down depending on the trend of the power consumption. If the electrical power consumption decreases after the change, the next pressure setpoint changes in the same way. If not, in the opposite way. In order to achieve these pressure setpoints, we used the pressure PID controllers tuned previously. Figure 10 shows the evolution of the high pressure during the optimization procedure.

The electrical power consumption of the plant decreases because of the optimization procedure, thus increasing the COP as expected with the optimization analysis of section 2.

Figure 10. Long term assay with the optimizer operation

## **7. CONCLUSIONS**

In this work, we derived and tested a real time optimization strategy for operation of transcritical CO<sub>2</sub> refrigeration plants. The main advantages of the proposed strategy are the use of a reduced number of measuring devices (a thermocouple, a pressure gauge and the power consumption of the plant obtained from the inverter drive), the independency on the refrigeration cycle and its components, its adaptability, and the guarantee of maximum efficiency operating conditions. An algorithm running in a programmable device implements the strategy. It includes two PI controllers for temperature and high-pressure tracking, its autotuning procedure, and a “perturb and observe” real-time optimization procedure. The algorithm decides the changes on the opening degree of the back-pressure valve and on the compressor speed from the measurements of the outlet temperature of the secondary fluid, the high-pressure and the power consumption. We tested the algorithm on a real plant, and observed the validity of the approach

We demonstrated that the maximization of the COP for CO<sub>2</sub> transcritical plants operating with constant thermal load is equivalent to the minimization of the electrical power consumption in the compressor, thus supporting mathematically the control algorithm. The proposal may be applicable to any CO<sub>2</sub> transcritical refrigeration plant just knowing some general parameters. The time required to make it work is lower than the one needed by other methods based on obtaining an experimental curve of the COP with respect to the high-pressure.

## **ACKNOWLEDGEMENTS**

The authors are indebted to the Spanish Ministry of Education and Science (CTM2008-06468-C02-02/TECNO) for the economic support given to the present work.

## REFERENCES

- [1] S. Girotto, S. Minetto, P. Neksa, Commercial refrigeration system using CO<sub>2</sub> as the refrigerant, *International Journal of Refrigeration*, 27 (2004) 717-723.
- [2] M.H. Kim, J. Pettersen, C.W. Bullard, Fundamental process and system design issues in CO<sub>2</sub> vapor compression systems, *Progress in Energy and Combustion Science*, 30 (2004) 119-174.
- [3] R. Cabello, D. Sánchez, R. Llopis, E. Torrella, Experimental evaluation of the energy efficiency of a CO<sub>2</sub> refrigerating plant working in transcritical conditions, *Applied Thermal Engineering*, 28 (2008) 1596-1604.
- [4] S.M. Liao, T.S. Zhao, A. Jakobsen, A correlation of optimal heat rejection pressures in transcritical carbon dioxide cycles, *Applied Thermal Engineering*, 20 (2000) 831-841.
- [5] J. Sarkar, S. Bhattacharyya, M.R. Gopal, Optimization of a transcritical CO<sub>2</sub> heat pump cycle for simultaneous cooling and heating applications, *International Journal of Refrigeration*, 27 (2004) 830-838.
- [6] S. Sawalha, Theoretical evaluation of trans-critical CO<sub>2</sub> systems in supermarket refrigeration. Part I: Modeling, simulation and optimization of two system solutions, *International Journal of Refrigeration*, 31 (2008) 516-524.
- [7] D. Sánchez, J. Patiño, R. Llopis, R. Cabello, E. Torrella, F.V. Fuentes, New positions for an internal heat exchanger in a CO<sub>2</sub> supercritical refrigeration plant. Experimental analysis and energetic evaluation, *Applied Thermal Engineering*, 63 (2014) 129-139.
- [8] D. Sánchez, J. Patiño, C. Sanz-Kock, R. Llopis, R. Cabello, E. Torrella, Energetic evaluation of a CO<sub>2</sub> refrigeration plant working in supercritical and subcritical conditions, *Applied Thermal Engineering*, <http://dx.doi.org/10.1016/j.applthermaleng.2014.02.005>.
- [9] Y.T. Ge, S.A. Tassou, Control optimisation of CO<sub>2</sub> cycles for medium temperature retail food refrigeration systems, *International Journal of Refrigeration*, 32 (2009) 1376-1388.
- [10] L. Cecchinato, M. Corradi, S. Minetto, A critical approach to the determination of optimal heat rejection pressure in transcritical systems, *Applied Thermal Engineering*, 30 (2010) 1812-1823.
- [11] N. Agrawal, S. Bhattacharyya, Optimized transcritical CO<sub>2</sub> heat pumps: Performance comparison of capillary tubes against expansion valves, *International Journal of Refrigeration*, 31 (2008) 388-395.
- [12] V. Casson, L. Cecchinato, M. Corradi, E. Fornasieri, S. Girotto, S. Minetto, L. Zamboni, C. Zilio, Optimisation of the throttling system in a CO<sub>2</sub> refrigerating machine, *International Journal of Refrigeration*, 26 (2003) 926-935.
- [13] C. Aprea, A. Maiorino, Heat rejection pressure optimization for a carbon dioxide split system: An experimental study, *Applied Energy*, 86 (2009) 2373-2380.

- [14] W.J. Zhang, C.L. Zhang, A correlation-free on-line optimal control method of heat rejection pressures in CO<sub>2</sub> transcritical systems, *International Journal of Refrigeration*, 34 (2011) 844-850.
- [15] S.S. Rao, *Engineering Optimization: Theory and Practice*, Hoboken, New Jersey, John Wiley & Sons, 2009.
- [16] S. Skogestad, I. Postlethwaite, *Multivariable feedback control: analysis and design*, Chichester, United Kingdom, John Wiley & Sons, 2005.
- [17] G.C. Goodwin, S.F. Graebe, M.E. Salgado, *Control system design*, New Jersey, EEUU, Prentice Hall, 2001.
- [18] D. Sánchez, E. Torrella, R. Cabello, R. Llopis, Influence of the superheat associated to a semihermetic compressor of a transcritical CO<sub>2</sub> refrigeration plant, *Applied Thermal Engineering*, 30 (2010) 302-309.
- [19] E. Torrella, D. Sánchez, R. Llopis, R. Cabello, Energetic evaluation of an internal heat exchanger in a CO<sub>2</sub> transcritical refrigeration plant using experimental data, *International Journal of Refrigeration*, 34 (2011) 40-49.
- [20] D. Sánchez, R. Cabello, R. Llopis, E. Torrella, Development and validation of a finite element model for water – CO<sub>2</sub> coaxial gas-coolers, *Applied Energy*, 93 (2012) 637-647.
- [21] R. Cabello, R. Llopis, D. Sánchez, E. Torrella, REFLAB: An Interactive Tool for Supporting Practical Learning in the Educational Field of Refrigeration, *International Journal of Engineering Education*, 27 (2011) 909 - 918.

## FIGURE CAPTIONS

Figure 1. Transcritical refrigeration CO<sub>2</sub> cycle with double expansion and P-h diagram

Figure 2. COP and equations ( 8 ) and ( 15 ) evolutions for  $P_o=35\text{bar}$  with  $R_{tot}=15^\circ\text{C}$  at two gas-cooler outlet temperatures

Figure 3. Scheme of the refrigeration plant, actuators, measured and control signals

Figure 4. Control scheme of the refrigeration plant

Figure 5. Possible schemes to regulate the secondary fluid outlet temperature and the power consumption of the refrigeration plant

Figure 6. Cascade structure for the controller and optimizer

Figure 7. Final control structure of the plant with the optimizer

Figure 8. View of the experimental plant and main actuators

Figure 9. Autotuning test for the PI controllers of the expansion valve and the compressor speed

Figure 10. Long term assay with the optimizer operation

## FIGURES

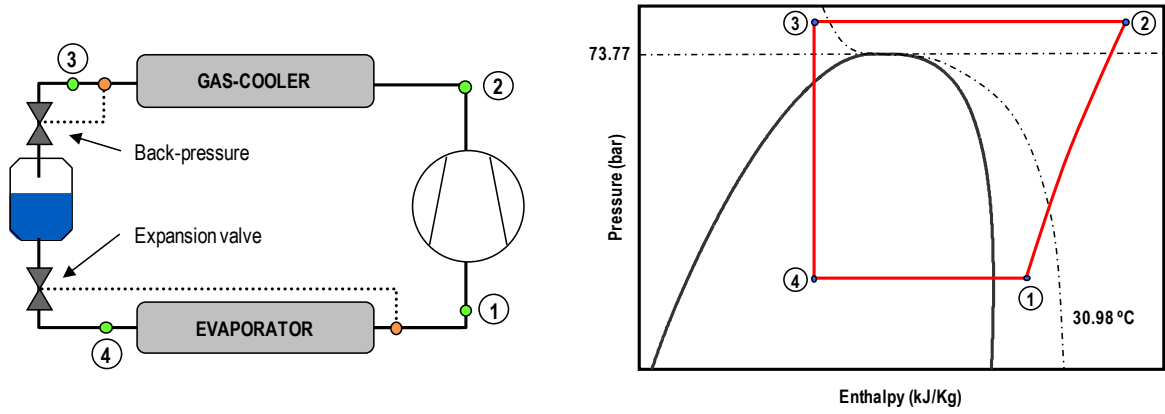


Figure 1. Transcritical refrigeration CO<sub>2</sub> cycle with double expansion and P-h diagram



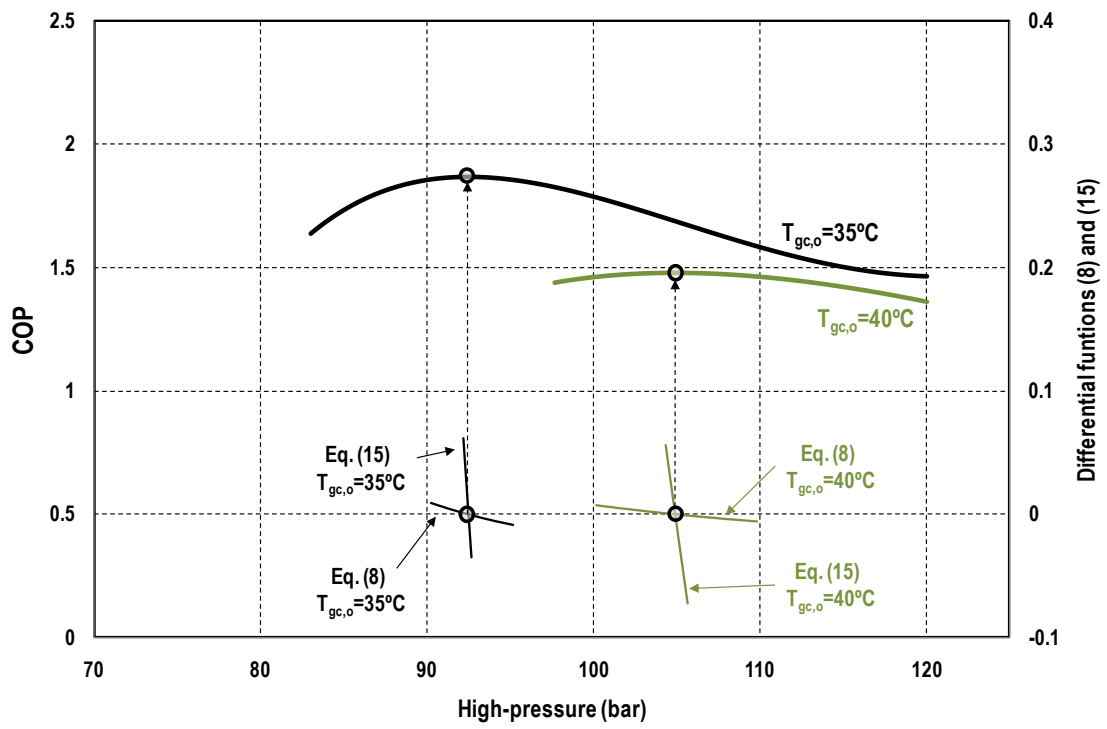


Figure 2. COP and equations ( 8 ) and ( 15 ) evolutions for  $P_o=35\text{bar}$  with  $R_{tot}=15^\circ\text{C}$  at two gas-cooler outlet temperatures

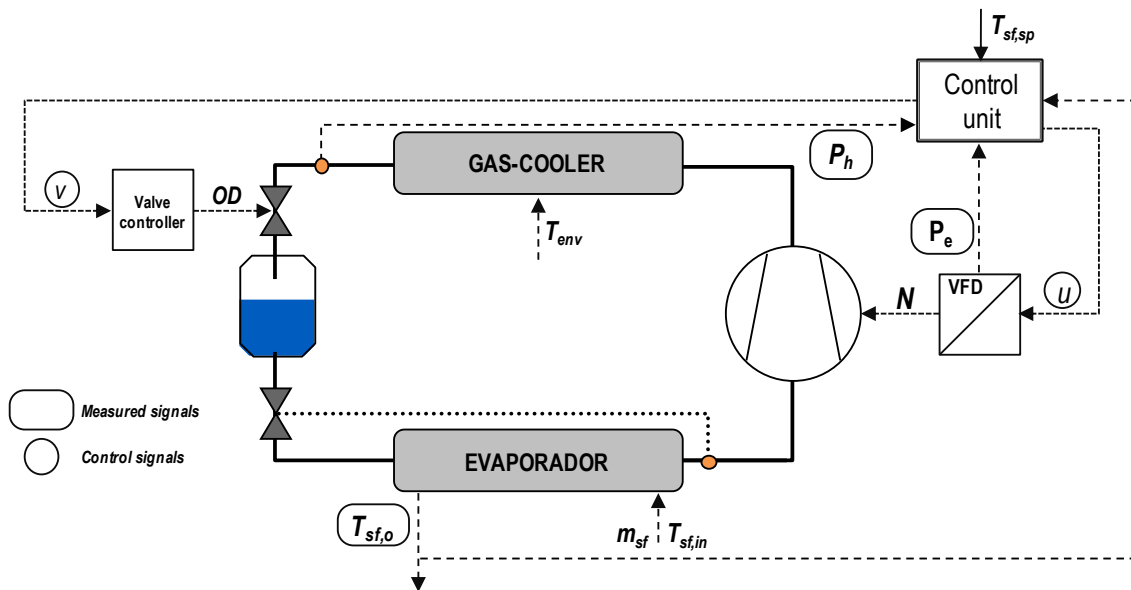


Figure 3. Scheme of the refrigeration plant, actuators, measured and control signals

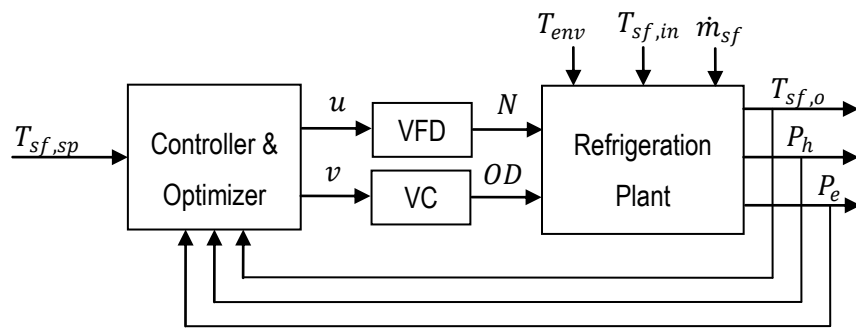


Figure 4. Control scheme of the refrigeration plant

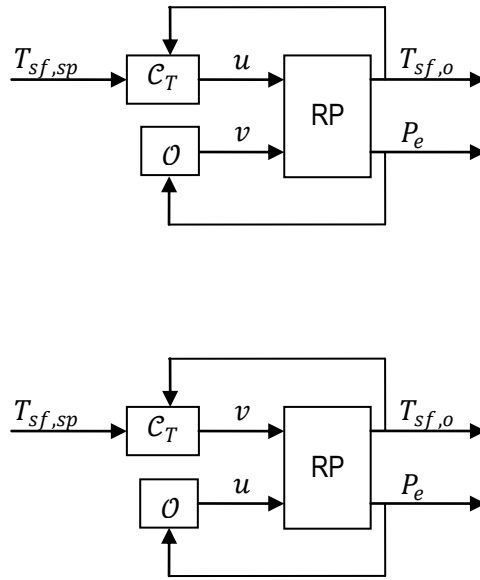


Figure 5. Possible schemes to regulate the secondary fluid outlet temperature and the power consumption of the refrigeration plant

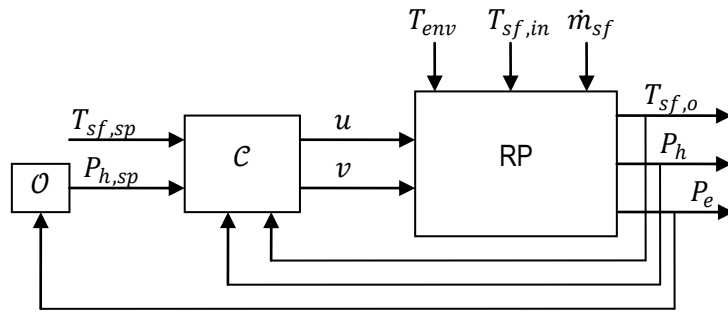


Figure 6. Cascade structure for the controller and optimizer

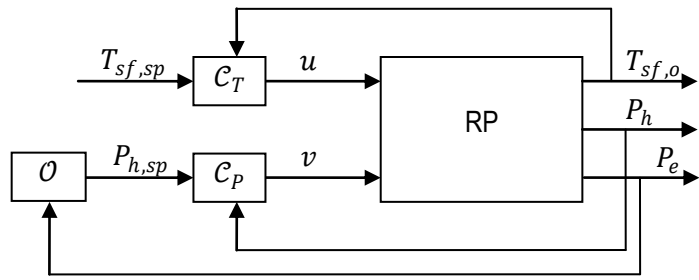


Figure 7. Final control structure of the plant with the optimizer

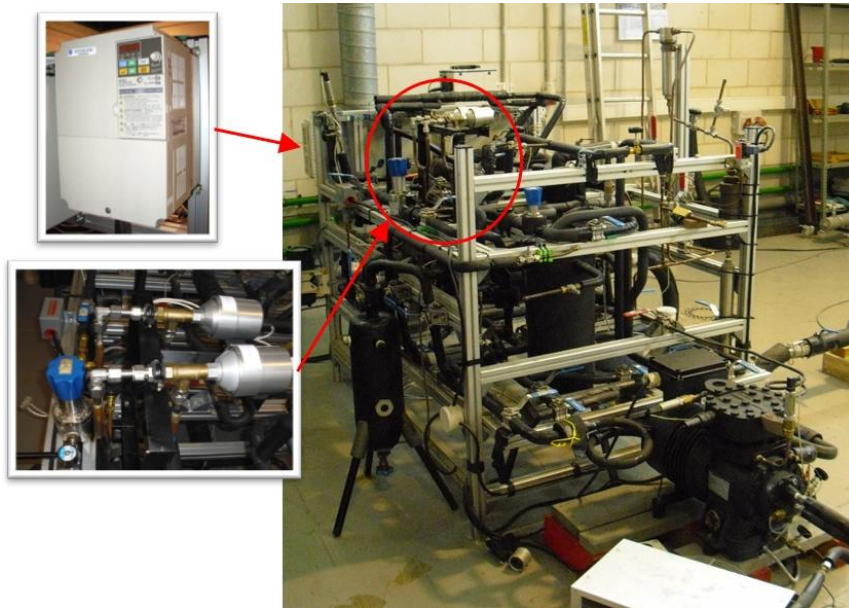


Figure 8. View of the experimental plant and main actuators

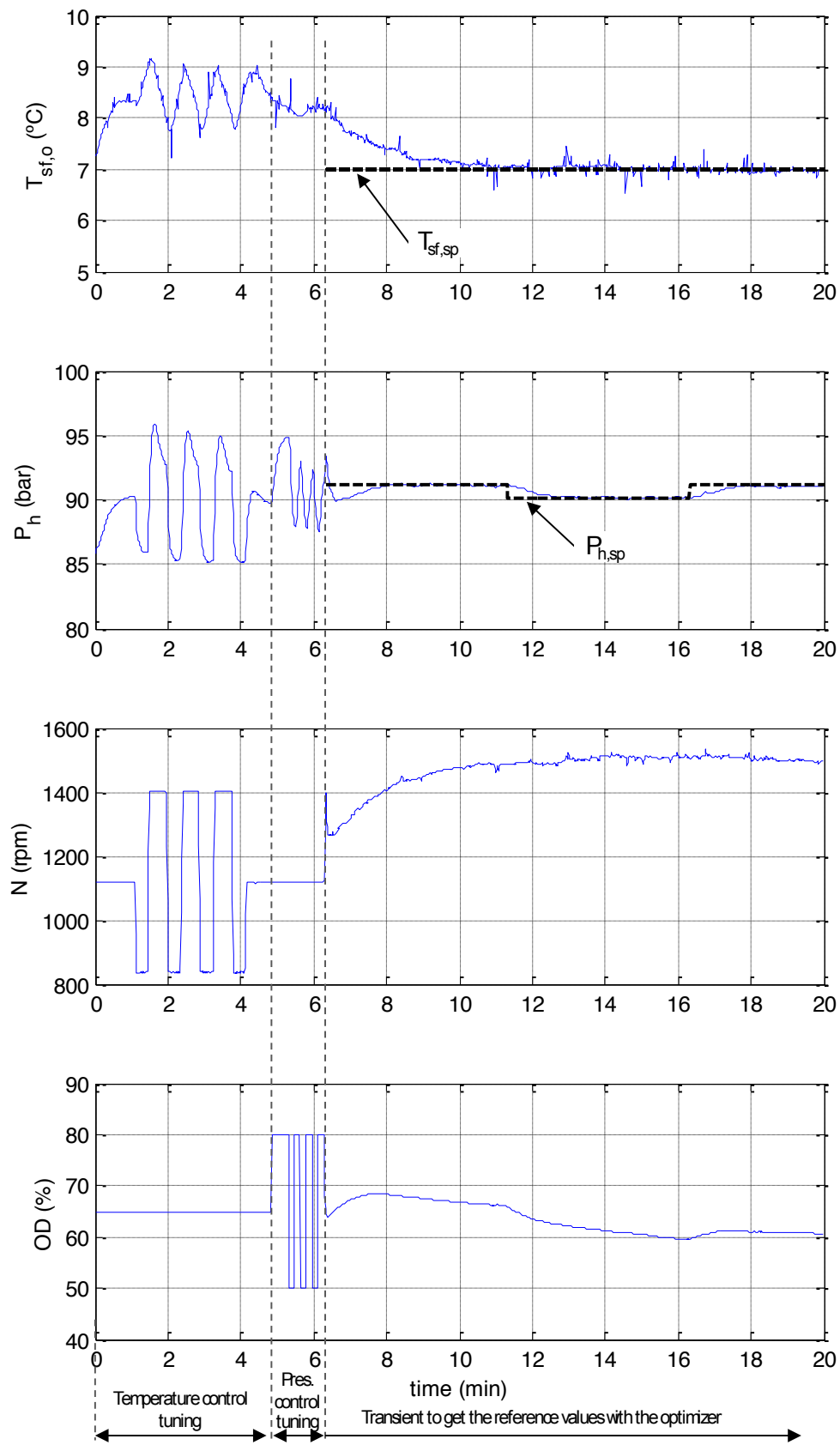


Figure 9. Autotuning test for the PI controllers of the expansion valve and the compressor speed



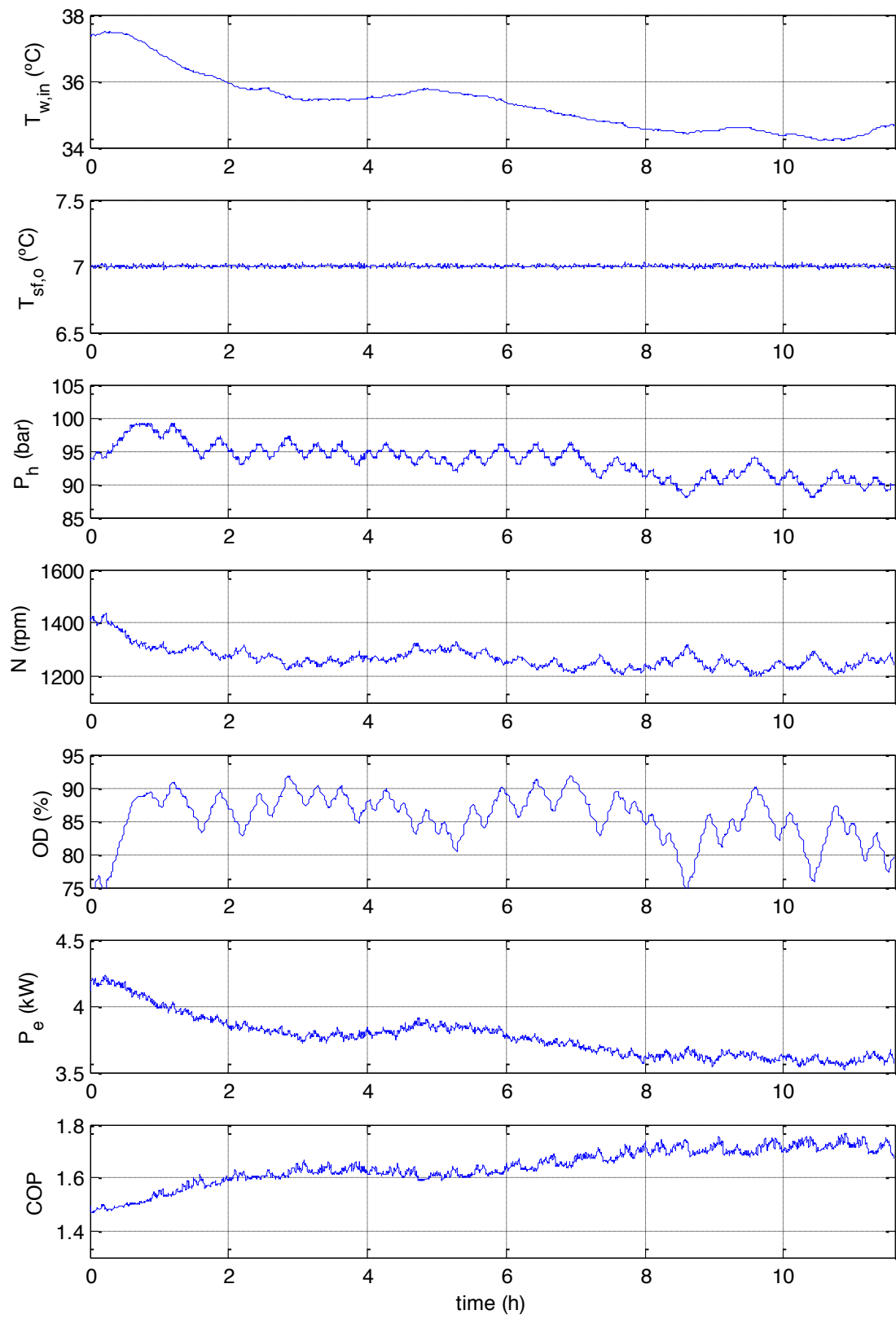


Figure 10. Long term assay with the optimizer operation